JCTC Journal of Chemical Theory and Computation

On the Dissociation of Ground State *trans*-HOOO Radical: A Theoretical Study

Josep M. Anglada,[†] Santiago Olivella,*[,†] and Albert Solé[‡]

Institut de Química Avançada de Catalunya, CSIC, Jordi Girona 18-26, 08034-Barcelona, Catalonia, Spain, and Departament de Química Física and Institut de Química Teòrica i Computacional, Universitat de Barcelona, Martí i Franquès 1, 08028-Barcelona, Catalonia, Spain

Received June 28, 2010

Abstract: The hydrotrioxyl radical (HOOO$^{\bullet}$) plays a crucial role in atmospheric processes involving the hydroxyl radical (HO$^{\bullet}$) and molecular oxygen (O_2). The equilibrium geometry of the electronic ground state (X ^{2}A″) of the *trans* conformer of HOOO$^{\bullet}$ and its unimolecular dissociation into HO$^{\bullet}$ (X $^2\Pi$) and O_2 (X $^3\Sigma_g^-$) have been studied theoretically using CASSCF and CASPT2 methodologies with the aug-cc-pVTZ basis set. On the one hand, CASSCF(19,15) calculations predict for *trans*-HOOO$^{\bullet}$ (X ^{2}A″) an equilibrium structure showing a central O−O bond length of 1.674 Å and give a classical dissociation energy $D_e = 1.1$ kcal/mol. At this level of theory, it is found that the dissociation proceeds through a transition structure involving a low energy barrier of 1.5 kcal/mol. On the other hand, CASPT2(19,15) calculations predict for *trans*-HOOO$^{\bullet}$ (X ^{2}A″) a central O−O bond length of 1.682 Å, which is in excellent agreement with the experimental value of 1.688 Å, and give $D_e = 5.8$ kcal/mol. Inclusion of the zero-point energy correction (determined from CASSCF(19,15)/aug-cc-pVTZ harmonic vibrational frequencies) in this D_e leads to a dissociation energy at 0 K of $D_0 = 3.0$ kcal/mol. This value of D_0 is in excellent agreement with the recent experimentally determined $D_0 = 2.9 \pm 0.1$ kcal/mol of Le Picard et al. (*Science* **2010**, *328*, 1258−1262). At the CASPT2 level of theory, we did not find for the dissociation of *trans*-HOOO$^{\bullet}$ (X ^{2}A″) an energetic barrier other than that imposed by the endoergicity of the reaction. This prediction is in accordance with the experimental findings of Le Picard et al., indicating that the reaction of HO$^{\bullet}$ with O_2 yielding HOOO$^{\bullet}$ is a barrierless association process.

1. Introduction

The hydrotrioxyl radical (HOOO$^{\bullet}$) is an important reactive intermediate of interest in many areas of chemistry, mainly in atmospheric chemistry.[1−23] Its equilibrium geometry, vibrational frequencies, reactivity, and the binding energy of the central O−O bond (designated by HO−OO$^{\bullet}$) have been the subject of numerous experimental and theoretical studies,[6,8−11,19,24−48] which have been recently summarized by Lester and co-workers.[49] The most important effect of HOOO$^{\bullet}$ in the Earth's atmosphere would arise if it could serve as a temporary sink for hydroxyl radicals (HO$^{\bullet}$) after their association with molecular oxygen (O_2).[50]

The first direct experimental observation of HOOO$^{\bullet}$ came from the work by Cacace et al.[32] using neutralization−reionization mass spectrometry, and it was subsequently observed by infrared spectroscopy in Ar and H_2O-ice matrices.[34] Spectroscopic observations of rotational transitions of HOOO$^{\bullet}$ and DOOO$^{\bullet}$ in the gas phase were made by Suma et al.[24] using Fourier-transform microwave (FTMW) spectroscopy. The determined rotational constants, as well as the ratio of *a*-type and *b*-type transition intensities, were consistent with a *trans* planar structure of ^{2}A″ character; however, the *cis* conformer was not observed. In conjunction with high-level multireference configuration interaction

* Corresponding author e-mail: sonqtc@cid.csic.es.
[†] Institut de Quimica Avançada de Catalunya.
[‡] Universitat de Barcelona.

10.1021/ct100358e
Published on Web 08/30/2010

(MRCI) calculations, the *A* and *B* rotational constants were used to determine an equilibrium geometry in which the HO−OO• bond length was 1.688 Å. Concerning the binding energy of this markedly long O−O bond, there has been much debate in the literature as to whether ground state (X ^{2}A″) of *trans*-HOOO• is sufficiently stable relative to the HO• (X $^2\Pi$) + O_2 (X $^3\Sigma_g^-$) dissociation limit to be present in measurable concentrations in the Earth's atmosphere. A full assessment of the atmospheric abundance of HOOO• requires detailed knowledge of its thermochemical properties. An indirect measurement of the stability of HOOO• was made by Speranza,[31] who inferred an enthalpy of formation of HOOO• of −1 ± 5 kcal/mol and consequently a HO−OO• bond dissociation enthalpy of 10 ± 5 kcal/mol. This value has since been re-examined by experiments reported by Lester and co-workers[1,2] using IR−UV double resonance spectroscopy to measure the HO• product state distribution following vibrational predissociation of HOOO•. From the energetically highest observed HO• product channel, an upper limit dissociation energy at 0 K (designated by D_0) of 6.12 kcal/mol was established for the HO−OO• bond.[1] An analogous study of the DOOO• isotopomer allowed this value to be refined and reduced the upper limit to 5.31 kcal/mol.[50] In addition, the latter value could be further improved if accurate zero-point vibrational energies for HOOO• and DOOO• were known.[51]

In comparing the experimentally determined upper limit of 5.31 kcal/mol for D_0 with the values obtained from theoretical calculations, the agreement between experimental and theoretical thermochemistry for HOOO• is poor. As noted by Varner et al.,[47] recent calculations of the D_0 in the *trans*-HOOO• conformer have begun to cluster around 1 to 3 kcal/mol, significantly below the experimental upper bound of 5.31 kcal/mol. One exception is the DFT calculations reported by Braams and Yu[42] based on the HCTH functional in conjunction with the aug-cc-pVTZ basis set, which predict $D_0 = 6.15$ kcal/mol. However, it should be pointed out that these HCTH/aug-cc-pVTZ calculations predict a HO−OO• bond length of 1.610 Å for *trans*-HOOO•, significantly shorter than the value of 1.688 Å derived from the experimental rotational constants.[24]

Varner et al.[47] have suggested that the apparent discrepancy between theory and experiment on the magnitude of the HO−OO• binding energy in the *trans*-HOOO• may be rationalized in terms of the existence of an exit barrier for the unimolecular dissociation. Using an equation-of-motion coupled-cluster singles and doubles method (designated by EOMIP-CCSD*) with the cc-pVQZ basis set, Varner et al.[47] investigated the dissociation profile of *trans*-HOOO• by computing the minimum energy for fixed values of the HO−OO• bond. In agreement with earlier theoretical studies[8,19,26,27,35] of the HOOO• dissociation to HO• + O_2, an exit barrier of approximately 3−5 kcal/mol was found. On the basis of when a barrier exists in a unimolecular decomposition pathway, highly nonstatistical behavior can occur; Varner et al.[47] suggest that it would seem plausible that perhaps 2 kcal/mol could be carried off by translational degrees of freedom. This would tend to greatly offset the difference between the theoretical D_0 value of 2−3 kcal/mol and the experimental upper limit of 5.31 kcal/mol determined by Lester and co-workers.[50]

During the preparation of this paper, Le Picard et al.[52] reported an experimental study on the decay of HO• radicals in the presence of O_2 at low temperatures (55.7−110.8 K) in a supersonic flow apparatus. Their study enabled the derivation of an experimental D_0 of 2.9 ± 0.1 kcal/mol, significantly below the experimental upper bound of 5.31 kcal/mol determined by Lester and co-workers.[50] In addition, the third-order rate constants for HOOO• formation determined in the study of Le Picard et al.[52] were found to have a strong negative temperature dependence, indicative of a barrierless association reaction. Therefore, there is a clear discrepancy between the experimental findings of Le Picard et al.[52] and the theoretical prediction of Varner et al.[47] concerning the existence of an exit barrier for the unimolecular dissociation of *trans*-HOOO• (X ^{2}A″) to HO• (X $^2\Pi$) + O_2 (X $^3\Sigma_g^-$).

Since it has been argued[10,11,24,41,42,44] that multireference-based methods are needed to correctly describe the electronic structure of HOOO•, the results of Varner et al.[47] motivated us to reinvestigate the minimum energy reaction path of *trans*-HOOO• (X ^{2}A″) dissociation to HO• (X $^2\Pi$) + O_2 (X $^3\Sigma_g^-$) using high level multireference-based methodologies. With this aim, herein, we report the results of CASSCF and CASPT2 electronic structure calculations on the equilibrium geometry of ground-state *trans*-HOOO• and its unimolecular dissociation.

2. Results and Discussion

2.1. CASSCF Approach. The calculations reported in this section were performed within the framework of the multiconfigurational self-consistent field (MCSCF) methodology of the complete active space (CAS) SCF class[53] employing Dunning's augmented correlation-consistent polarized valence triple-ζ (aug-cc-pVTZ) basis set.[54] For *trans*-HOOO•, all 19 valence electrons were distributed in all possible ways in the active space generated following the procedure suggested by Anglada and Bofill,[55] based on the fractional occupation of the natural orbitals generated from the first-order density matrix calculated from an initial multireference single- and double-excitation configuration interaction (MRDCI) wave function correlating all valence electrons. These indicated a CAS of 15 orbitals (11 a′ and 4 a″) and led to a CASSCF wave function, designated by CASSCF(19,15), formed as a linear combination of 6 246 240 doublet spin-adapted configuration state functions (CSFs). This CASSCF wave function has already been used with the 6-311+G(2df,2p) basis set in a recent[41] theoretical study on the nature of the long O−O bond in HOOO•. For the dissociation products of *trans*-HOOO• (X ^{2}A″), the aforementioned active space selection procedure indicated a number of active orbitals that varied from seven, for HO• (X $^2\Pi$), to eight, for O_2 (X $^3\Sigma_g^-$). The distribution among these active orbitals of the corresponding number of valence electrons led to the CASSCF wave functions denoted by CASSCF(7,7) and CASSCF(12,8), respectively.

Table 1. Relative Energies[a] (kcal/mol) and Geometrical Parameters[b] (distances in Å and angles in deg) of the Relevant Stationary Points on the Ground-State Potential Energy Surface for the Dissociation of *trans*-HOOO$^{\bullet}$ (X ^{2}A″) to HO$^{\bullet}$ (X $^2\Pi$) + O_2 (X $^3\Sigma_g^-$) Calculated at the CASSCF(19,15)/aug-cc-pVTZ Level

species	ΔU	ΔE_0	$r(O_aO_b)$	$r(O_bO_c)$	$r(O_cH)$	$\theta(O_aO_bO_c)$	$\theta(O_bO_cH)$	$\tau(O_aO_bO_cH)$
trans-HOOO$^{\bullet}$	0.0	0.0	1.226	1.674	0.973	109.9	96.9	180.0
TS	1.5	0.1	1.214	2.128	0.974	112.0	90.5	176.4
CX	0.9	−1.4	1.217	2.894	0.974	114.0	84.9	179.6
HO$^{\bullet}$ + O_2	1.1	−1.7	1.218		0.974			

[a] ΔU is the relative electronic energy, and ΔE_0 is the ZPVE-corrected relative energy. [b] Geometrical parameters defined as in Figure 1.

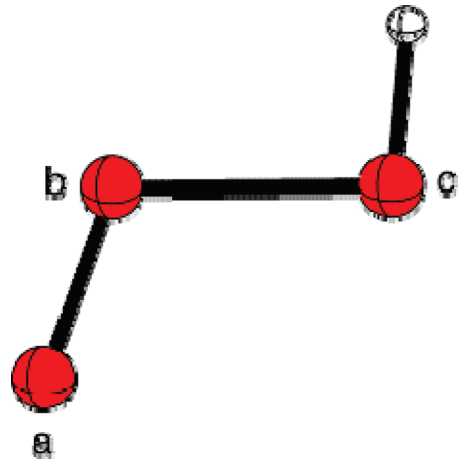

Figure 1. Optimized equilibrium structure of *trans*-HOOO$^{\bullet}$ (X ^{2}A″).

The geometries of the relevant stationary points (minima and first-order saddle points) on the lowest-energy potential energy surface (PES) of the dissociation of *trans*-HOOO$^{\bullet}$ (X ^{2}A″) to HO$^{\bullet}$ (X $^2\Pi$) + O_2 (X $^3\Sigma_g^-$) were optimized at the CASSCF(19,15) level of theory by using analytical gradients procedures.[56] The harmonic vibrational frequencies of these stationary points were computed at the same level of theory. Zero-point vibrational energies (ZPVEs) were determined from unscaled CASSCF(19,15) harmonic vibrational frequencies. All of the CASSCF calculations were carried out using the GAMESS[57] program package.

In Table 1, we present the relative electronic energies (designated by ΔU), the ZPVE-corrected relative energies (designated by ΔE_0), and geometrical parameters of the stationary points (see Figure 1 for atom labeling). The calculated harmonic vibrational frequencies are compared with the vibrational frequencies measured from the experimental IR spectra in Table S4 (Supporting Information). Overall, the geometrical parameters computed for *trans*-HOOO$^{\bullet}$ compare well with the values determined from the experimental rotational constants in conjunction with MRCI calculations.[24] In particular, the HO−OO$^{\bullet}$ bond length ($r(O_bO_c)$) of 1.674 Å and the terminal O−O bond length ($r(O_aO_b)$) of 1.226 Å are in good agreement with the experimental values of 1.688 and 1.225 Å, respectively.[24] However, the $\theta(O_bO_cH)$ bond angle is calculated to be 6.9° larger than the experimental value of 90.0°. On the other hand, our CASSCF(19,15) calculations largely underestimate the binding energy of the HO−OO$^{\bullet}$ bond. That is, whereas the ΔU data listed in Table 1 indicate that *trans*-HOOO$^{\bullet}$ lies 1.1 kcal/mol below the energy of HO$^{\bullet}$ (X $^2\Pi$) + O_2 (X $^3\Sigma_g^-$), the calculated ΔE_0 data show that *trans*-HOOO$^{\bullet}$ is 1.7 kcal/mol more energetic than the dissociation products. These results are in clear disagreement with the most recent experimental D_0 of 2.9 ± 0.1 kcal/mol.[52]

Table 2. A Comparison of Barrier Heights (in kcal/mol) Calculated for the Dissociation of HOOO$^{\bullet}$ into HO$^{\bullet}$ + O_2

method	$\Delta U^{\ddagger}$[a]	$\Delta E_0^{\ddagger}$[b]	$\Delta H^{\ddagger}$ (298 K)[c]	ref
CASSCF(3,3)	4			26
MCHF	16.5			27
QCISD(T)-CBS	8.9			35
B3LYP			3.7	19
CCSD(T)-CBS(W1U)	6.6	5.3		8
EOMIP-CCSD*	3−4			47
CASSCF(19,15)	1.5	0.1		this work

[a] Potential energy barrier. [b] Energy barrier at 0 K. [c] Enthalpy barrier at 298 K.

Our CASSCF(19,15) calculations predict that the dissociation of *trans*-HOOO$^{\bullet}$ (X ^{2}A″) to HO$^{\bullet}$ (X $^2\Pi$) + O_2 (X $^3\Sigma_g^-$) proceeds via a transition structure. The geometrical parameters computed for this transition structure, labeled as **TS**, are shown in Table 1. From the geometry point of view, the main feature of **TS** is the long $r(O_bO_c)$ distance of 2.128 Å. The ΔU data listed in Table 1 show that the dissociation of *trans*-HOOO$^{\bullet}$ involves a potential energy barrier (designated by $\Delta U^{\ddagger}$) of 1.5 kcal/mol. Inclusion of ZPVE corrections to energy leads to an energy barrier at 0 K (designated by $\Delta E_0^{\ddagger}$) of only 0.1 kcal/mol. These barrier heights are compared in Table 2 with the values found in previous theoretical studies. In particular, it is remarkable that the $\Delta U^{\ddagger}$ of 1.5 kcal/mol computed at the CASSCF(19,15) level is much lower than the $\Delta U^{\ddagger}$ of 6.6 kcal/mol reported by Fabian et al.[8] based on CCSD(T)-CBS (W1U) calculations and significantly lower than the $\Delta U^{\ddagger}$ of approximately 3−4 kcal/mol estimated by Varner et al.[47] at the EOMIP-CCSD* level. This is attributed to the fact that both CCSD(T)-CBS (W1U) and EOMIP-CCSD* are correlated single-reference-based methods, which take into account the dynamic electron correlation effects, whereas CASSCF(19,15) is a multiconfigurational method, which takes into account the near degeneracy effects in the electronic structure (i.e., the nondynamic electron correlation).

Intrinsic reaction coordinate calculations[58] showed that **TS** goes backward to *trans*-HOOO$^{\bullet}$ and goes forward to give a product complex in which the HO$^{\bullet}$ radical is loosely bound to the O_2. The optimized geometry of this complex, labeled as **CX**, was characterized as a true local minimum on the PES. There is no classical barrier for the dissociation of **CX** into HO$^{\bullet}$ (X $^2\Pi$) + O_2 (X $^3\Sigma_g^-$) other than that imposed by the endoergicity of the process. The relative energies and geometrical parameters computed for **CX** are shown in Table 1. The ΔU data listed in Table 1 show that **CX** lies 0.9 kcal/

Table 3. Classical Dissociation Energy (D_e, in kcal/mol), Dissociation Energy at 0 K (D_0 in kcal/mol), and Geometrical Parameters[a] (distances in Å and angles in deg) Calculated at Different CASPT2 Levels with the aug-cc-pVTZ Basis Set for *trans*-HOOO$^\bullet$ (X ^{2}A″)

method	D_e	D_0	$r(O_aO_b)$	$r(O_bO_c)$	$r(O_cH)$	$\theta(O_aO_bO_c)$	$\theta(O_bO_cH)$	$\tau(O_aO_bO_cH)$
CASPT2(13,11)	5.4	2.6[b]	1.214	1.734	0.973	110.7	95.2	180.0
CASPT2(19,15)	5.8	3.0[b]	1.221	1.682	0.971	110.2	95.8	180.0
exp[c]		2.9 ± 0.1	1.225	1.688	0.972	111.0	90.0	180.0

[a] Geometrical parameters defined as in Figure 1. [b] ZPVE-correction evaluated from the unscaled CASSCF(19,15)/aug-cc-pVTZ harmonic vibrational frequencies. [c] Experimental geometrical parameters from ref 24 and experimental D_0 from ref 52.

mol above the energy of *trans*-HOOO$^\bullet$ and 0.2 kcal/mol below the energy of the isolated dissociation products HO$^\bullet$ (X $^2\Pi$) and O_2 (X $^3\Sigma_g^-$). Inclusion of ZPVE corrections to energy changes the relative energy ordering of these stationary points. Thus, according to the calculated ΔE_0 values, **CX** is found to be 1.4 kcal/mol below the energy of *trans*-HOOO$^\bullet$ but 0.3 kcal/mol above the energy of the dissociation products. These results lessen the importance of the possible existence of a loosely bound complex **CX** in the exit channel of the unimolecular dissociation of *trans*-HOOO$^\bullet$ (X ^{2}A″) to HO$^\bullet$ (X $^2\Pi$) + O_2 (X $^3\Sigma_g^-$).

We note that the present CASSCF calculations predict that the unimolecular dissociation of *trans*-HOOO$^\bullet$ (X ^{2}A″) to HO$^\bullet$ (X $^2\Pi$) + O_2 (X $^3\Sigma_g^-$) proceeds through an exit channel involving a low energy barrier. This prediction is at variance with the experimental findings of Le Picard et al.,[52] indicating that the inverse reaction, namely, the association of HO$^\bullet$ and O_2 yielding HOOO$^\bullet$, occurs over a minimum potential energy path with no barrier between the reactants HO$^\bullet$ + O_2 and the product HOOO$^\bullet$.

2.2. CASPT2 Approach. The calculations reported in this section were performed within the framework of the second-order multiconfigurational perturbation theory based on a CASSCF reference wave function (CASPT2)[59] employing an IPEA shift[60] of 0.25 au, as implemented in the MOLCAS-7.4 suite of programs,[61] in conjunction with the aug-cc-pVTZ basis set. Two CASs of different sizes were used in the CASSCF reference function of the CASPT2 calculations. First, a reduced valence electron CASSCF reference wave function for *trans*-HOOO$^\bullet$ was generated by distributing the valence electrons excluding six inner electrons (seeded in the 2s atomic orbitals of the three oxygen atoms) among the active orbitals determined by using the above procedure. This indicated a CAS of 11 orbitals (7 a′ and 4 a″) and led to a reference CASSCF wave function, designated by CASSCF-(13,11), formed as a linear combination of 76 230 doublet spin-adapted CSFs. For each dissociation product, the small reference CASSCF wave function was generated by distributing the corresponding valence electrons (excluding the electrons seeded in the 2s atomic orbitals of the oxygen atoms) among the active orbitals generated according to the aforementioned procedure, which resulted in five active orbitals for HO$^\bullet$ (X $^2\Pi$) and six active orbitals for O_2 (X $^3\Sigma_g^-$). This led to the CASSCF reference wave functions denoted by CASSCF(5,5) and CASSCF(8,6), respectively. Second, the all valence electron CASSCF(19,15), CASSCF-(7,7), and CASSCF(12,8) wave functions described above for *trans*-HOOO$^\bullet$ (X ^{2}A″), HO$^\bullet$ (X $^2\Pi$), and O_2 (X $^3\Sigma_g^-$), respectively, were taken as the larger CASSCF reference wave functions employed in the CASPT2 calculations. For the sake of brevity, the different CASPT2 levels of calculation are designated by CASPT2(m,n), where m is the number of electrons and n the number of orbitals of the CASSCF reference wave function.

Table 4. A Comparison of Classical Dissociation Energies (D_e, in kcal/mol), Dissociation Energies at 0 K (D_0, in kcal/mol), and Central O−O Bond Lengths ($r(O_bO_c)$, in Å) Calculated for HOOO$^\bullet$

method	D_e	D_0	$r(O_bO_c)$	ref
MCHF	13.8		1.472	27
G2M2(RCC)		1.3	1.543	30
MRMP2//CASSCF	6.0	2.8	1.750	11
QCISD(T)-CBS	5.3		1.495	35
CCSD(T)-CBS(W1U)	3.4	0.1	1.544	8
MRCIQ+Q	3.9		1.677	24
CCSD(T)//QCISD	0.1	−3.9	1.522	41
MRCI+Q	5.4	1.4	1.647	41
MRCI+Q//CASSCF	3.5		1.544	42
HCTH	9.9	6.2	1.610	42
CCSD(T)	5.2	2.5	1.589	47
CASPT2(13,11)	5.4	2.6	1.734	this work
CASPT2(19,15)	5.8	3.0	1.682	this work
exp		2.9 ± 0.1	1.688	24,[a] 52[b]

[a] Experimental $r(O_bO_c)$. [b] Experimental D_0.

The geometries were optimized using gradients determined through a finite difference of CASPT2 energies. The values of the classical dissociation energy (designated by D_e) and D_0, along with the geometrical parameters, calculated for *trans*-HOOO$^\bullet$ (X ^{2}A″) at the CASPT2(13,11) and CASPT(19,15) levels are summarized in Table 3. The unscaled CASSCF-(19,15) harmonic vibrational frequencies were used to compute the ZPVE corrections to obtain D_0 from D_e. For the purpose of comparison, the values of D_e, D_0, and $r(O_bO_c)$ calculated for HOOO$^\bullet$ by several previous theoretical studies are collected in Table 4.

The optimized geometrical parameters of the equilibrium structure computed at the CASPT2(13,11) level for *trans*-HOOO$^\bullet$ are in relatively good agreement with the values determined from the experimental rotational constants in conjunction with MRCI calculations.[24] In the case of the HO−OO$^\bullet$ bond, the $r(O_bO_c)$ of 1.734 Å appears to be 0.046 Å longer than the experimental value of 1.688 Å.[24] Fortunately, the most expensive calculation reported here (i.e., the full CASPT2(19,15) geometry optimization) predicts an $r(O_bO_c)$ of 1.682 Å, in excellent agreement with the experimental value. For the rest of the geometrical parameters, the values calculated at the CASPT2(19,15) level are similar to those obtained at the less expensive CASPT2(13,11) level. Concerning the dissociation energies, it appears (see Table 3) that the values of D_e and D_0 calculated at the CASPT2(19,15) level are 0.4 kcal/mol larger than those

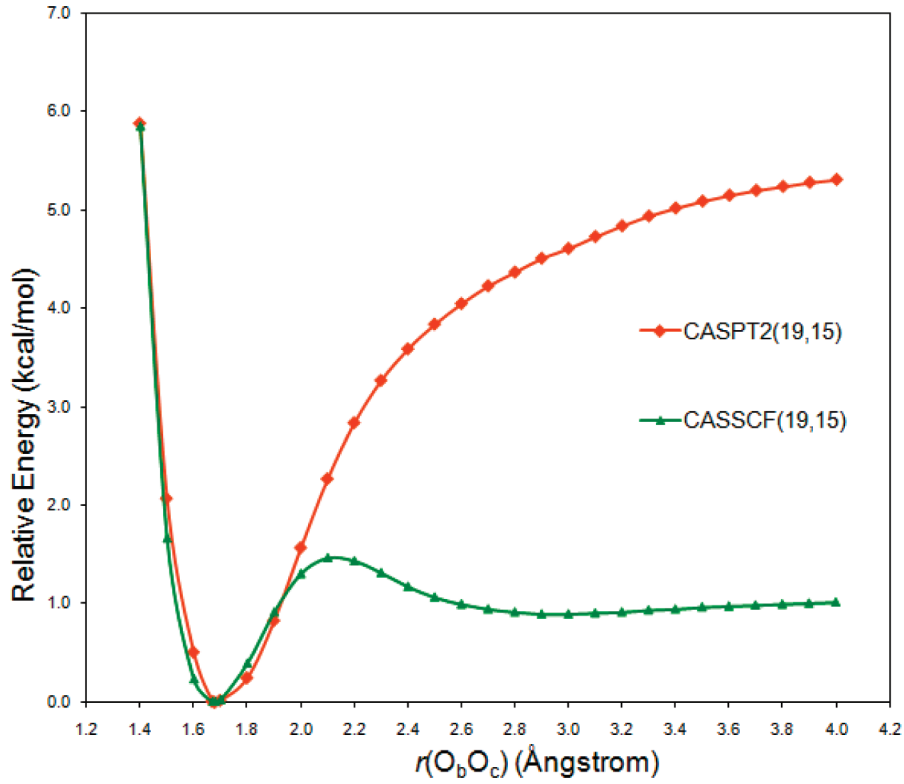

Figure 2. Potential energy profiles for dissociation of *trans*-HOOO$^{\bullet}$ (X ^{2}A″) to HO$^{\bullet}$ (X $^2\Pi$) + O_2 (X $^3\Sigma_g^-$) calculated at two different levels of theory along the $r(O_bO_c)$ coordinate using geometries optimized at the CASSCF(19,15)/aug-cc-pVTZ level.

computed at the CASPT2(13,11) level. Furthermore, we note that the $D_e = 5.8$ and $D_0 = 3.0$ kcal/mol predicted by our CASPT2(19,15) calculations are about 0.5 kcal/mol higher than the theoretical $D_e = 5.2$ and $D_0 = 2.5$ kcal/mol values obtained recently by Varner et al.[47] using high-level coupled-cluster methods. In comparison with experimental values, though the CASPT2(19,15) computed $D_0 = 3.0$ kcal/mol is approximately 2.3 kcal/mol below the D_0 upper bound of 5.31 kcal/mol,[62] it is gratifying to note that our theoretical value is in excellent agreement with the most recent experimentally determined $D_0 = 2.9 \pm 0.1$ kcal/mol.[52]

To investigate the minimum energy reaction path of *trans*-HOOO$^{\bullet}$ (X ^{2}A″) dissociation into HO$^{\bullet}$ (X $^2\Pi$) + O_2 (X $^3\Sigma_g^-$), potential energy profiles were calculated along the $r(O_bO_c)$ coordinate at different levels of theory. First, the geometries were optimized at the CASSCF(19,15)/aug-cc-pVTZ level for all degrees of freedom except a fixed $r(O_bO_c)$ distance that increased at 0.1 Å intervals. In addition, CASPT2(19,15)/aug-cc-pVTZ single-point energy calculations were performed for the geometries optimized at the CASSCF(19,15) level of theory. The resulting graphs of the potential energy profiles are shown in Figure 2. We note that at both levels of theory a minimum exists on the ground-state dissociation profile of *trans*-HOOO$^{\bullet}$ (^{2}A″). Starting from the minimum, at the CASSCF(19,15) level of theory, the *trans*-HOOO$^{\bullet}$ (^{2}A″) surmounts a very low energy barrier (ca. 1.5 kcal/mol) at $r(O_bO_c) = 2.1$ Å, which corresponds to the transition structure **TS** described above. A shallow potential energy well is observed at $r(O_bO_c) = 2.9$ Å, which corresponds to the loosely bound complex **CX** described above. In clear contrast, the graph of the dissociation profile calculated at the CASPT2(19,15) level of theory shows that the potential energy of *trans*-HOOO$^{\bullet}$ (^{2}A″) increases smoothly until it reaches asymptotically the dissociation limit HO$^{\bullet}$ (X $^2\Pi$) + O_2 (X $^3\Sigma_g^-$) without surmounting any energy barrier other than that imposed by the endoergicity of the dissociation.

Second, the geometries were optimized at 0.1 Å intervals for the $r(O_bO_c)$ distance at the CASPT2(13,11)/aug-cc-pVTZ level. The reoptimization of these geometries at the CASPT2(19,15)/aug-cc-pVTZ level was not attempted in the present study due to the prohibitive computational cost involved.[63] Nevertheless, as noted above, except for the $r(O_bO_c)$ distance, the geometrical parameters optimized at the CASPT2(19,15) level for *trans*-HOOO$^{\bullet}$ (X ^{2}A″) are close to those obtained at the less expensive CASPT2(13,11) level. Therefore, CASPT2(19,15)/aug-cc-pVTZ single-point energy calculations were performed for the geometries optimized at the CASPT2(13,11) level of theory. The resulting graphs of the potential energy profiles are shown in Figure 3. Again, the graphs of the dissociation profile calculated at either the CASPT2(13,11) or CASPT2(19,15) level of theory show that the potential energy of *trans*-HOOO$^{\bullet}$ (^{2}A″) increases smoothly until it reaches asymptotically the dissociation limit HO$^{\bullet}$ (X $^2\Pi$) + O_2 (X $^3\Sigma_g^-$) without surmounting any energy barrier. Consequently, according to the more reliable multireference CASPT2 method, no reverse activation energy is involved in this dissociation. This prediction is in accordance with the experimental findings of Le Picard et al.,[52] indicating that the reaction of HO$^{\bullet}$ with O_2 yielding HOOO$^{\bullet}$ is a barrierless association process.

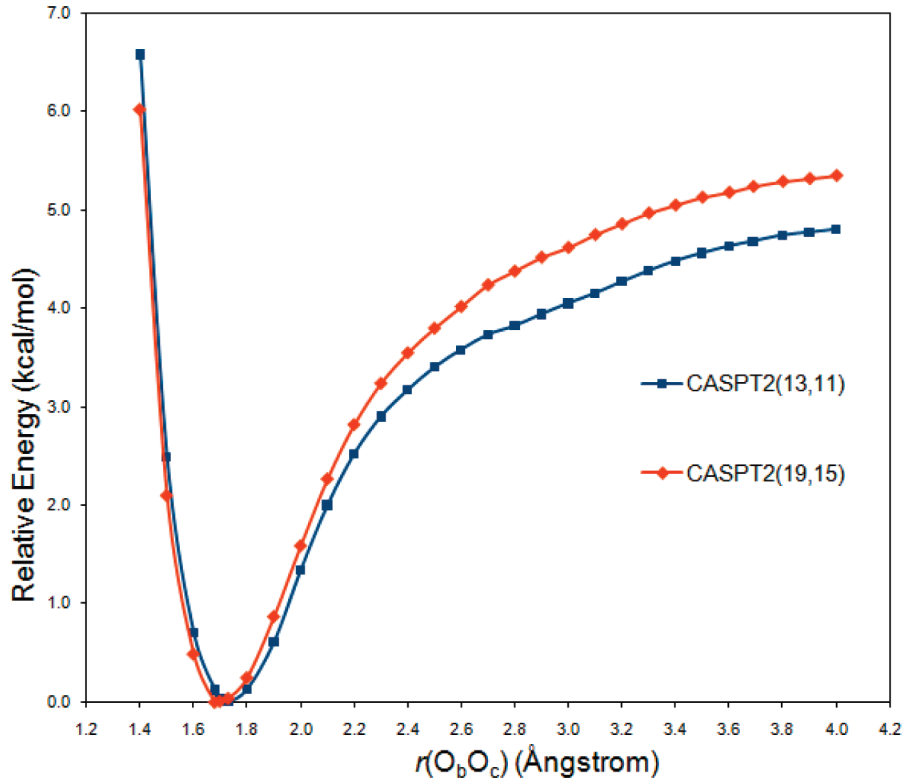

Figure 3. Potential energy profiles for dissociation of *trans*-HOOO$^{\bullet}$ (X ^{2}A″) to HO$^{\bullet}$ (X $^2\Pi$) + O_2 (X $^3\Sigma_g^-$) calculated at two different CASPT2 levels along the $r(O_bO_c)$ coordinate using geometries optimized at the CASPT2(13,11)/aug-cc-pVTZ level.

3. Summary and Conclusions

Quantum-mechanical multireference-based methods CASSCF and CASPT2 were employed with the aug-cc-pVTZ basis set to investigate the equilibrium geometry of the electronic ground state of *trans*-HOOO$^{\bullet}$ (^{2}A″) and its unimolecular dissociation into HO$^{\bullet}$ (X $^2\Pi$) and O_2 (X $^3\Sigma_g^-$). From the analysis of the results, the following main points emerge.

The CASSCF(19,15) calculations predict for *trans*-HOOO$^{\bullet}$ (X ^{2}A″) an equilibrium structure with a HO−OO$^{\bullet}$ bond length of 1.674 Å, which is in reasonable agreement with the experimental value of 1.688 Å, and give a small classical dissociation energy $D_e = 1.1$ kcal/mol. Inclusion of the ZPVE corrections leads to a 0 K dissociation energy $D_0 = -1.7$ kcal/mol, which is grossly in disagreement with the recent experimentally determined $D_0 = 2.9 \pm 0.1$ kcal/mol by Le Picard et al.

At the CASSCF(19,15) level of theory, it is found that the dissociation of *trans*-HOOO$^{\bullet}$ (X ^{2}A″) into HO$^{\bullet}$ (X $^2\Pi$) and O_2 (X $^3\Sigma_g^-$) proceeds through a transition structure involving a low energy barrier of 1.5 kcal/mol. This theoretical prediction is at variance with the experimental findings of Le Picard et al., indicating that the inverse reaction, namely, the association of HO$^{\bullet}$ and O_2 yielding HOOO$^{\bullet}$, occurs over a minimum potential energy path with no barrier between the reactants HO$^{\bullet}$ + O_2 and the product HOOO$^{\bullet}$.

The most reliable calculation performed in this work, a full geometry optimization of *trans*-HOOO$^{\bullet}$ (X ^{2}A″) at the CASPT2(19,15)/aug-cc-pVTZ level, gives a HO−OO$^{\bullet}$ bond length of 1.682 Å, which is in excellent agreement with the experimental value. At this level of theory, D_e is calculated to be 5.8 kcal/mol. Inclusion of the zero-point energy correction (determined from CASSCF(19,15)/aug-cc-pVTZ harmonic vibrational frequencies) to this D_e leads to $D_0 = 3.0$ kcal/mol. This value of D_0 is in excellent agreement with the recent experimentally determined $D_0 = 2.9 \pm 0.1$ kcal/mol by Le Picard et al.

At the CASPT2(13,11) and CASPT2(19,15) levels of theory, we did not find for the dissociation of *trans*-HOOO$^{\bullet}$ (X ^{2}A″) a barrier other than that imposed by the endoergicity of the reaction. Consequently, no reverse activation energy is involved in this dissociation. This prediction is in accordance with the experimental findings of Le Picard et al., indicating that the reaction of HO$^{\bullet}$ with O_2 yielding HOOO$^{\bullet}$ is a barrierless association process.

Overall, it can be concluded that the quantum-mechanical multireference-based method CASPT2 correctly describes both the electronic structure of *trans*-HOOO$^{\bullet}$ (^{2}A″) and its unimolecular dissociation into HO$^{\bullet}$ (X $^2\Pi$) and O_2 (X $^3\Sigma_g^-$).

Acknowledgment. This research was supported by the Spanish MICINN (Grant CTQ2008-06536/BQU). Additional support came from the Catalonian AGAUR (Grant 2009SGR01472). The larger calculations described in this work were performed at the Centre de Supercomputació de Catalunya (CESCA).

Supporting Information Available: The total energies, zero-point vibrational energies, harmonic vibrational frequencies, and Cartesian coordinates of all structures reported in this paper. This material is available free of charge via the Internet at http://pubs.acs.org.

References

(1) Murray, C.; Derro, E. L.; Sechler, T. D.; Lester, M. I. *J. Phys. Chem. A* **2007**, *111*, 4727.

(2) Derro, E. L.; Murray, C.; Sechler, T. D.; Lester, M. I. *J. Phys. Chem. A* **2007**, *111*, 11592.

(3) Chalmet, S.; Ruiz-Lopez, M. F. *J. Chem. Phys.* **2006**, *124*, 194502.

(4) Chin, G. *Science* **2003**, *302*, 535.

(5) Cooper, P. D.; Moore, M. H.; Hudson, R. L. *J. Phys. Chem. A* **2006**, *110*, 7985.

(6) Yu, H.-G.; Varandas, A. J. C. *J. Chem. Soc., Faraday Trans.* **1997**, *93*, 2651.

(7) Szichman, H.; Varandas, A. J. C. *J. Phys. Chem. A* **1999**, *103*, 1967.

(8) Fabian, W. N. F.; Kalcher, J.; Janoschek, R. *Theor. Chem. Acc.* **2005**, *114*, 182.

(9) Varandas, A. J. C. *J. Phys. Chem. A* **2004**, *108*, 758.

(10) Yang, J.; Li, Q. S.; Zhang, S.-W. *Phys. Chem. Chem. Phys.* **2007**, *9*, 466.

(11) Setokuchi, O.; Sato, M.; Matuzawa, S. *J. Phys. Chem. A* **2000**, *104*, 3204.

(12) Cerkovnik, J.; Erzen, E.; Koller, J.; Pleniscar, B. *J. Am. Chem. Soc.* **2002**, *124*, 404.

(13) Le Crane, J. P.; Rayez, J. C.; Villanave, E. *Phys. Chem. Chem. Phys.* **2006**, *8*, 2163.

(14) Srinivasan, N. K.; Su, M. C.; Sutherland, J. V.; Michael, J. V. *J. Phys. Chem. A* **2005**, *109*, 7902.

(15) Wentworth, P.; Jones, L. H.; Wentworth, A. D.; Zhu, X. Y.; Larsen, N. A.; Wilson, I. A.; Xu, X.; Goddard, W. A.; Janda, K. D.; Eschenmoser, A. *Science* **2001**, *293*, 1806.

(16) Pleniscar, B.; Cerkovnik, J.; Takavec, T.; Koller, J. *Chem.—Eur. J.* **2000**, *6*, 809.

(17) Pleniscar, B. *Acta Chim. Slov.* **2005**, *52*, 1.

(18) Engdahl, A.; Nelander, B. *Science* **2002**, *295*, 482.

(19) Xu, X.; Goddard, W. A. *Proc. Natl. Acad. Sci. U. S. A.* **2002**, *96*, 15308.

(20) Alosio, S.; Francisco, J. S. *J. Am. Chem. Soc.* **1999**, *121*, 8592.

(21) Kraka, E.; Cremer, D.; Koller, J.; Pleniscar, B. *J. Am. Chem. Soc.* **2002**, *124*, 8462.

(22) Chalmet, S.; Ruiz-Lopez, M. F. *ChemPhysChem* **2006**, *7*, 463.

(23) Wu, A.; Cremer, D.; Pleniscar, B. *J. Am. Chem. Soc.* **2003**, *125*, 9395.

(24) Suma, K.; Sumiyoshi, Y.; Endo, Y. *Science* **2005**, *308*, 1885.

(25) Blint, R. J.; Newton, M. D. *J. Phys. Chem.* **1973**, *59*, 6220.

(26) Mathisen, K. B.; Siegbahn, P. E. M. *Chem. Phys.* **1984**, *90*, 225.

(27) Dupuis, M.; Fitzgerald, G.; Hammond, B.; Leister, W. A.; Schaefer, H. F., III. *J. Chem. Phys.* **1986**, *84*, 2691.

(28) Vincent, M. A.; Hillier, I. H.; Burton, N. A. *Chem. Phys. Lett.* **1995**, *233*, 111.

(29) Speranza, M. *Inorg. Chem.* **1996**, *35*, 6140.

(30) Jungkamp, T. P. W.; Seinfeld, J. H. *Chem. Phys. Lett.* **1996**, *257*, 15.

(31) Speranza, M. *J. Phys. Chem. A* **1998**, *102*, 7535.

(32) Cacace, F.; de Petris, G.; Pepi, F.; Troiani, A. *Science* **1999**, *285*, 81.

(33) Hollebeek, T.; Ho, T. S.; Rabitz, H. *Annu. Rev. Phys. Chem.* **1999**, *50*, 537.

(34) Nelander, B.; Engdahl, A.; Svensson, T. *Chem. Phys. Lett.* **2000**, *332*, 403.

(35) Yu, H.-G.; Varandas, A. J. C. *Chem. Phys. Lett.* **2001**, *334*, 173.

(36) Pei, K. M.; Zhang, X. Y.; Kong, X. L.; Li, H. Y. *Chin. J. Chem. Phys.* **2002**, *15*, 263.

(37) Denis, P. A.; Kieninger, M.; Ventura, O. N.; Cachau, R. E.; Diercksen, G. H. F. *Chem. Phys. Lett.* **2002**, *365*, 440. Erratum **2003**, *377*, 483.

(38) Varandas, A. C. J. *Chem. Phys. Chem.* **2005**, *3*, 453.

(39) Janoschek, R.; Fabian, W. M. F. *J. Mol. Struct.* **2006**, *780*, 80.

(40) Xu, Z. F.; Lin, M. C. *Chem. Phys. Lett.* **2007**, *440*, 12.

(41) Mansergas, A.; Anglada, J. M.; Olivella, S.; Ruiz-Lopez, M. F.; Martins-Costa, M. *Phys. Chem. Chem. Phys.* **2007**, *9*, 5865.

(42) Braams, B. J.; Yu, H.-G. *Phys. Chem. Chem. Phys.* **2008**, *10*, 3150.

(43) Varner, M. E.; Harding, M. E.; Gauss, J.; Stanton, J. F. *Chem. Phys.* **2008**, *346*, 53.

(44) Semes'ko, D. G.; Khursan, S. L. *Russ. J. Phys. Chem. A* **2008**, *82*, 1277.

(45) Denis, P. A.; Ornellas, F. R. *Chem. Phys. Lett.* **2008**, *464*, 150.

(46) Denis, P. A.; Ornellas, F. R. *J. Phys. Chem. A* **2009**, *113*, 499.

(47) Varner, M. E.; Harding, M. E.; Vazquez, J.; Gauss, J.; Stanton, J. F. *J. Phys. Chem A* **2009**, *113*, 11238.

(48) Grant, D. J.; Dixon, D. A.; Francisco, J. S.; Feller, D.; Peterson, K. A. *J. Phys. Chem. A* **2009**, *113*, 11343.

(49) Murray, C.; Derro, E. L.; Sechler, T.-D.; Lester, M. I. *Acc. Chem. Res.* **2009**, *42*, 419.

(50) Derro, E. L.; Sechler, T. D.; Murray, C.; Lester, M. I. *J. Phys. Chem. A* **2008**, *112*, 9269.

(51) Derro, E. L.; Sechler, T. D.; Murray, C.; Lester, M. I. *J. Chem. Phys.* **2008**, *128*, 244313.

(52) Le Picard, S. D.; Tizniti, M.; Canosa, A.; Sims, I. R.; Smith, I. W. M. *Science* **2010**, *328*, 1258.

(53) For a review, see: Roos, B. O. *Adv. Chem. Phys.* **1987**, *69*, 399.

(54) Kendall, R. A.; Dunning, T. H., Jr.; Harrison, R. J. *J. Chem. Phys.* **1992**, *96*, 6796.

(55) Anglada, J. M.; Bofill, J. M. *Theor. Chim. Acta* **1995**, *92*, 369.

(56) (a) Schlegel, H. B. *J. Comput. Chem.* **1982**, *3*, 214. (b) Bofill, J. M. *J. Comput. Chem.* **1994**, *15*, 1.

(57) Schmidt, M. W.; Baldrige, K. K.; Boatz, J. A.; Elbert, S. T.; Gordon, M. S.; Jensen, J.; Koseki, S.; Matsunaga, N.; Nguyen, K. A.; Su, S.; Windus, T. L.; Dupuis, M.; Montgomery, J. A. *J. Comput. Chem.* **1993**, *14*, 1347.

(58) (a) Gonzalez, C.; Schlegel, H. B. *J. Chem. Phys.* **1989**, *90*, 2154. (b) Gonzalez, C.; Schlegel, H. B. *J. Phys. Chem.* **1990**, *94*, 5523.

(59) (a) Anderson, K.; Malmqvist, P.-A.; Roos, B. O.; Sadlej, A. J.; Wolinski, K. *J. Phys. Chem.* **1990**, *94*, 5483. (b) Anderson, K.; Malmqvist, P.-A.; Roos, B. O. *J. Chem. Phys.* **1992**, *96*, 1218.

(60) Ghigo, G.; Roos, B. O.; Malmqvist, P.-Å. *Chem. Phys. Lett.* **2004**, *396*, 142.

(61) Karlström, G.; Lindh, R.; Malmqvist, P.-Å.; Roos, B. O.; Ryde, U.; Veryazov, V.; Widmark, P.-O.; Cossi, M.; Schimmelpfennig, B.; Neogrády, P.; Seijo, L. *Comput. Mater. Sci.* **2003**, *28*, 222.

(62) At this point, it is worth pointing out that this upper bound value of D_0 was determined for the DOOO$^\bullet$ isotopomer.[50] Derro et al.[51] suggested that a reduced value of D_0 is expected for HOOO$^\bullet$ because the ZPVEs of HOOO$^\bullet$ and HO$^\bullet$ are likely to be larger than those of DOOO$^\bullet$ and DO$^\bullet$, respectively. In fact, we have calculated the ZPVEs of DOOO$^\bullet$ and DO$^\bullet$ at the CASSCF(19,15)/aug-cc-pVTZ level of theory (see Table S2, Supporting Information). The resulting values, in conjunction with the ZPVE of O_2, give a Δ(ZPVE) of -2.3 kcal/mol for the dissociation of DOOO$^\bullet$, which is 0.5 kcal/mol larger than the value of -2.8 kcal/mol calculated at the same level of theory for the dissociation of HOOO$^\bullet$. The estimated *corrected* experimental D_0 upper bound value of HOOO$^\bullet$ is, thus, 5.3 $-$ 0.5 kcal/mol, namely, 4.8 kcal/mol.

(63) It takes about 400 h of CPU time to perform a single point calculation of the energy plus energy gradients at the CASPT2(19,15)/aug-cc-pVTZ level on a 3.0 GHz Intel Xeon E5472 CPU.

CT100358E